Final Draft
of the original manuscript:

Zotzmann, J.; Behl, M.; Feng, Y.; Lendlein, A.:
Copolymer Networks Based on Poly(Omega-pentadecalactone) and Poly(Epsilon-caprolactone)Segments as a Versatile Triple-Shape Polymer System
In: Advanced Functional Materials (2010) Wiley

DOI: 10.1002/adfm.201000478

Submitted to ADVANCED FUNCTIONAL MATERIALS

DOI: 10.1002/adfm.((please insert DOI)

Copolymer Networks Based on Poly(ω-pentadecalactone)- and Poly(ε-caprolactone)-Segments as a versatile Triple-Shape Polymer System

By *Jörg Zotzmann*, *Marc Behl*, *Yakai Feng*, and *Andreas Lendlein**

[*] Prof. A. Lendlein, Corresponding-Author
Centre of Biomaterial Development, Institute of Polymer Research, GKSS Research Center Geesthacht GmbH
Kantstr. 55, D-14513 Teltow (Germany)
E-mail: lendlein@gkss.de
Fax: +49 3328 352452

Dr. J. Zotzmann, Dr. M. Behl, Dr. Y. Feng[1]
Centre of Biomaterial Development, Institute of Polymer Research, GKSS Research Center Geesthacht GmbH
Kantstr. 55, D-14513 Teltow (Germany)

[1]present address: Tianjin University, Department of Polymer Science and Technology
92 Weijin Road, Tianjin 300072 (China)

Submitted to ADVANCED FUNCTIONAL MATERIALS

Abstract:
Triple-shape polymers can perform two consecutive shape changes in response to heat. These shape changes correspond to the recovery of two different deformations in reversed order, which were programmed before at elevated temperature levels (T_{mid} and T_{high}) by application of external stress. Recently, an AB copolymer network was described, which surprisingly exhibited a triple-shape effect although being programmed with only one deformation at T_{high}. We explored whether a copolymer network system could be designed enabling a one-step deformation process at ambient temperature (cold drawing) as a novel gentle and easy-to-handle triple-shape creation procedure in addition to the to date reported procedures, which generally involve deformation(s) at elevated temperature(s). A copolymer network system with two crystallizable polyester segments was synthesized and characterized fulfilling two crucial criteria. These materials could be deformed at ambient temperature by cold drawing and showed even at T_{high}, which was above the melting points of both switching domains, elongations at break of up to 250%. Copolymer networks with a PCL content of 75 and 50 wt% showed a triple-shape effect after cold drawing with shape-fixity ratios between 65% and 80% and total shape recovery ratio above 97%. Furthermore, in these copolymer networks a triple-shape effect could be obtained after one-step deformation at T_{high}. Independent from the temperature at which the deformation was applied (ambient temperature or T_{high}), copolymer networks having the same compositions showed similar switching temperatures and proportioning of the contribution during recovery in two steps. The two-step programming procedure enabled a triple-shape effect in copolymer networks for an even broader range of compositions. This versatile triple-shape material system based on tailored building blocks is an interesting candidate material for applications in fixation systems or disassembling systems.

Keywords: Polymer Networks, Shape-Memory Effect, Stimuli-Sensitive Polymers, Triple-Shape Effect, Cold Drawing

1. Introduction

Shape-memory polymers (SMP) are actively moving polymers with the capability of changing their shape in a predefined way when triggered by an external stimulus such as temperature.[1-3] In a process called programming the SMP is heated to a temperature above the transition temperature T_{trans} associated to its switching domains and deformed. While keeping the external stress, the polymer is cooled to a temperature below T_{trans} causing the switching domains to solidify and the temporary shape is fixed.[4-7] The original, permanent shape is recovered by reheating and driven by entropy elasticity. Multiphase polymer networks having two switching domains can store and subsequently memorize two shape-changes resulting in polymers with a thermally-induced triple-shape effect (TSE).[8, 9] Triple-shape polymers can switch from a first temporary shape (A) to a second temporary shape (B) and from there to the permanent shape (C) when heated. The thermal transitions associated to the switching domains can be glass transitions ($T_{trans} = T_g$) or melting points ($T_{trans} = T_m$).[10] A macroscopic TSE could as well be obtained as multimaterial system by combination of two dual-shape materials in a bilayer system.[11] In this paper we focus on single material systems.

A two-step programming process (2SPP) was applied in order to create the two temporary shapes (A) and (B) of the polymer network.[8] 2SPP starts from the permanent shape (C) with a first deformation at T_{high}, which is above both T_{trans} associated to the switching domains, and subsequent cooling to a temperature T_{mid}, which is between $T_{trans,1}$ and $T_{trans,2}$, while the external stress was maintained resulting in the fixation of shape (B). A second deformation performed at T_{mid} and subsequent cooling to a temperature T_{low}, which is below both T_{trans} results in the temporary shape (A). In multiphase polymer networks the temporary shapes are fixed by physical crosslinks, which are established during cooling while the permanent shape (C) is defined by the covalent crosslinks established during the synthesis. When the programmed sample is reheated the stored deformations are recovered.

Two different polymer network architectures could be realized by photo-induced copolymerization of a methacrylate monomer and a dimethacrylate as crosslinker. The AB copolymer network system, named MACL, consists of poly(cyclohexyl methacrylate) chains crosslinked by poly(ε-caprolactone) (PCL) segments. MACL polymer networks exhibited a T_m at 50 °C and a T_g at 140 °C to be used as the two T_{trans}s required for TSE. Here, both types of polymer chain segments form links between netpoints and contribute in this way to the overall macroscopic elasticity of the polymer network. A different polymer network architecture was obtained by incorporation of poly(ethylene glycol)-segments (PEG-segments) as side chains having one dangling end into a PCL network. In this copolymer network with grafted side chains named CLEG the PCL segments dominantly determined the overall macroscopic elasticity.[12] Both segments are crystallizable so that both switching domains are related to T_ms. In-situ x-ray scattering studies revealed that low-melting PCL crystallites were supporting the PEG crystallites in the fixation of shape (A) in CLEG polymer networks.[13] In a similar approach, TSE was realized in a system based on high density polyethylene blended with polyethylene having different degrees of branching, which was crosslinked after blending.[9] A linear multiblock copolymers obtained from three different building blocks, enabled a TSE in a thermoplastic material.[14] Recently, Tao Xie reported a TSE and quadruple-shape effect in commercially available NAFION®, an amorphous thermoplast, having a very broad thermal transition.[15]

A notable phenomenon was observed for MACL polymer networks. Although only a single-step deformation was applied at T_{high} during programming a TSE was observed during reheating.[16] For this purpose the material was deformed at T_{high} to an elongation ε^0_A and cooled to T_{low} whereby stress is kept constant, resulting in shape (A) after unloading of the stress. The triple-shape capability after application of this programming method named one-

step programming procedure (1SPP) could be obtained as both switching segments were oriented when the polymer network was sufficiently deformed.

We explored whether a copolymer network system could be designed enabling the programming of a TSE by a one-step deformation process at ambient temperature (cold drawing) in addition to 2SPP and 1SPP. This novel triple-shape creation procedure, which we named c1SPP, would greatly improve the triple-shape technology as the time interval for the programming could be significantly shortened. Furthermore, limitations based on low mechanical toughness at T_{high} as well as thermal degradation potentially occurring during programming could be avoided. However, a key requirement for materials suitable of c1SPP is their ability to be deformed by cold drawing. MACL-based polymer networks are brittle at ambient temperature having elongations at break (ε_b) below 20% and CLEG-based polymer networks in the composition range capable of exhibiting a TSE can be deformed to 100%, but did not show a TSE.[10] Therefore, a novel copolymer network had to be created. In the design of such polymers we were inspired by the observation that multiblock copolymers based on poly(pentadecalactone) (PPD) and PCL blocks displayed high values of ε_b at room temperature (above 300%) and enabled cold-drawing to create a dual-shape effect.[17, 18] We synthesized a copolymer network system based on these two crystallizable segments by crosslinking star-shaped hydroxy-telechelic PPD and PCL precursors with a low-molecular weight diisocyanate. This synthesis route was selected as polyesterurethane networks having one switching domain were investigated extensively as multifunctional dual-shape materials before.[19-22] The network architecture of the synthesized copolymer networks is sketched in **Fig. 1**, in which the polymer network chain segments can be built by linking two hydroxy-terminated oligomer arms of the same kind or a mixed pair.

The thermal and mechanical properties of the copolymer networks were investigated under variation of two molecular parameters, the molecular weight of the star-shaped precursors as

well as the weight fraction of the two polymer segments in the networks. In this way we explored whether the two T_ms are well-separated and whether the copolymer networks can be deformed sufficiently at T_{high} as well as at ambient temperature. Copolymer networks fulfilling the thermal and mechanical requirements will be investigated with regard to their triple-shape capabilities by applying the three different programming procedures 2SPP, 1SPP, and c1SPP. The contribution of the two switching segments on the shape-fixity ratio and the shape-recovery ratio will be determined with regard to their composition. From these results function-property relationships will be derived.

As polymer networks containing a crystallizable segments displayed a reversible shape-changing effect due to crystallization induced elongation (CIE) and melting induced contraction when subjected to a constant external stress[23] we investigated the copolyesterurethane networks containing two crystallizable segments with PPD and PCL with regard to a reversible TSE, the results of which are reported in reference[24].

Insert Figure 1 here.

2. Results and discussion

Polymer networks were obtained by crosslinking star-shaped precursors with TMDI (mixture of the two isomers 1,6-diisocyanato-2,2,4-trimethylhexane and 1,6-diisocyanato-2,4,4-trimethylhexane) in a polyaddition reaction catalyzed by dibutyl tindilaurate (DBTDL).[21, 25]

The star-shaped hydroxy-telechelic precursors T^3PPD(5), T^3PPD(3), P^4PCL(18), and P^4PCL(5) were synthesized by ring-opening polymerization (ROP) from the cyclic monomers ω-pentadecalactone (PDL) respectively ε-caprolactone (CL) using dibutyl tinoxide (DBTO) as catalyst.[24] Star-shaped precursors are named in the following according to the initiator and the number of hydroxy functionalities (three arm PPD precursor – T^3PPD, and four arm PCL

precursors – P^{4}PCL) with approximate values of M_n (obtained from gel permeation chromatography (GPC) measurements) x·1000 g·mol^{-1} given in parenthesis. Quantities of the reactants in ROP as well as M_n, T_g, and T_m of the resulting precursors are summarized in supporting information Table S1.

Six sets of copolymer networks (containing both segments) were synthesized differing in the M_n of the precursors used as starting materials. Within these sets of copolymer networks the content of P^{4}PCL (μ_{PCL}) in the synthesis reaction was varied between 25 wt% and 75 wt%. Additionally, the homopolymer network from each single precursor was synthesized in order to investigate the influence of the polymer chain length on the thermal and mechanical properties in the homopolymer networks and to compare it with the tendencies occurring in the copolymer networks. Quantities of the reactants in polymer network synthesis are summarized in supporting information Table S2.

The results from swelling experiments in chloroform and the thermal properties of the polymer networks are listed in **Tab. 1**. The gel content (G) of all polymer networks resulted in values between 91 and 99% indicating an almost complete crosslinking reaction with the exception of a few polymer networks incorporating P^{4}PCL(18), which exhibited slightly lower gel contents because of a decreased accessibility of the OH-groups due to enhanced coiling of the PCL-arms.[24]

Insert Table 1 here.

Thermal analysis was performed to investigate, if the two amorphous phases are miscible since the crystallization processes of the switching segment would potentially be affected by this. For this purpose the T_g determined for the copolymer networks will be compared to the T_gs of the homopolymer networks. Furthermore, it is investigated whether the two T_ms

associated to the two switching domains are separated sufficiently. A minimum temperature difference of about 20 K between the two T_ms is desirable in order to separate two shape changes. This temperature difference might be influenced by the polymer network chain segment length and the interaction of both segments with each other. Furthermore, 2SPP and 1SPP (as well as reversible TSE) require two distinct crystallization temperatures (T_c) for the fixation of two distinct temporary shapes. This is of minor importance when a TSE by c1SPP should be obtained as no fixation by crystallization is involved.

A sufficient fixation capability of each polymer segment is substantially determined by the degree of crystallinity. The contribution of the segments could be estimated by comparison of the values of the melting enthalpy ($\Delta_m H$). The overall degree of crystallinity was determined by x-ray scattering, while the distribution of the crystallites of both polymer segments was visualized by polarized optical microscopy (POM). The question, which copolymer network compositions enable sufficient shape-fixation was finally explored by the cyclic, thermomechanical experiments. In addition to the thermal properties the mechanical properties were determined depending of the programming temperature in order to investigate the deformability of the polymer networks at different temperature levels.

In differential scanning calorimetry (DSC) measurements a T_g could be determined only for the PCL homopolymer networks and in the copolymer networks T-T^{3}PPD(5)P^{4}PCL(10,75), T-T^{3}PPD(5)P^{4}PCL(10,60), and T-T^{3}PPD(5)-P^{4}PCL(5,75) having a PCL content of more than 50 wt% (see Tab. 1). Quenching by fast cooling in DSC did not lead to a sufficient decrease in crystallinity so that this experiment did also not offer more insight in the thermal transition of the amorphous domains.[26] In order to detect T_gs of copolymer networks having a broader range of PCL content dynamic mechanical analysis at varied temperature (DMTA) measurements were conducted for the copolymer networks from the P^{4}PCL(18) series in which a $T_{g,PCL}$ between -60 and -55 °C as well as very broad T_g between -30 and 0 °C could

be detected. This indicates the existence of an amorphous (dominantly) PCL phase while the occurrence of a mixed PCL/PPD phase related to a T_g above -30 °C could not be excluded due to the broadness, given the information $T_{g,PPD}$ = -30 °C.

In DSC measurements the PCL-based homopolymer networks showed a PCL melting point ($T_{m,PCL}$) between 32 and 53 °C, which was a function of length of the polymer chain segments (controlled by M_n) of the PCL precursors (Fig. 2A upper box). The PPD homopolymer networks exhibited a $T_{m,PPD}$ decreasing from of 81 to 71 °C from T-T^{3}PPD(5) to T-T^{3}PPD(3). Conclusively, a sufficient difference in the T_ms of the two segments can be expected for the copolymer networks. All copolymer networks exhibited two distinct melting ranges except the copolymer networks T-T^{3}PPD(x)P^{4}PCL(5,25) where no $T_{m,PCL}$ could be detected due to the short PCL chains combined with the low PCL content. In the copolymer networks $T_{m,PPD}$ varied between 63 and 79 °C and $T_{m,PCL}$ between 27 and 55 °C showing the same dependence from M_n of the precursors (**Fig. 2A** lower box) but no systematic dependence from μ_{PCL}. $T_{m,PPD}$ slightly decreased with increasing PCL content in all six series of copolymer networks. This was attributed to a constrained crystal formation due to a lower mobility of the chain segments at increased crosslinking density, as T^{3}PPD precursors were substituted by P^{4}PCL precursors. For all copolymer networks showing two T_ms both T_ms were separated by at least 20 K with the exception of the T-T^{3}PPD(3)P^{4}PCL(18,y) series. The T-T^{3}PPD(3)P^{4}PCL(5,y) series showed $T_{m,PCL}$ in the range of room temperature, which is disadvantageous for shape-fixation in c1SPP. Furthermore, most copolymer networks from the T-T^{3}PPD(3)P^{4}PCL(10,y) and the T-T^{3}PPD(3)P^{4}PCL(5,y) series exhibited two $T_{c,PPD}$ with the lower one overlapping with $T_{c,PCL}$. This second $T_{c,PPD}$ indicated a mixed amorphous phase of PPD and PCL, which demixed below the first $T_{c,PPD}$ and led to a second PPD crystallization so that it is very unlikely to store two distinct temporary shapes in these copolymer networks. In addition to the small difference between the two T_ms of the T-T^{3}PPD(3)P^{4}PCL(18,y) series this was the

reason that all three copolymer network series based on T-T^{3}PPD(3) were not investigated further. A strong influence of μ_{PCL} on T_c of PPD could be observed. The copolymer network T-T^{3}PPD(5)P^{4}PCL(18,75) incorporating only 25 wt% PPD showed no $T_{c,PPD}$, while in the copolymer networks T-T^{3}PPD(5)P^{4}PCL(18,60), T-T^{3}PPD(5)P^{4}PCL(10,75) and T-T^{3}PPD(5)P^{4}PCL(5,75) $T_{c,PPD}$ was decreased by 14 to 36 K compared to the copolymer networks within the same series. The influence of the cooling rate on the T_cs in the copolymer networks was investigated by applying cooling rates of 50, 20, 10, 5, 2, 1, and 0.5 K·min^{-1} on the T-T^{3}PPD(5)P^{4}PCL(10,50). $T_{c,PCL}$ was increasing from 8 to 31 °C and $T_{c,PPD}$ from 44 to 68 °C. However, the difference between both T_cs remained almost constant at 37 K, so that for the thermomechanical measurements the maximum cooling rate of 5 K·min^{-1} was chosen.

The values of $\Delta_m H_{PCL}$ and $\Delta_m H_{PPD}$ were not decreasing with decreasing content of the respective polymer segment (**Fig. 2B**) leading to the assumption that the extent of crystallinity contributed by each of the polymer segments was a nearly linear function of μ_{PCL}.

Insert Figure 2 here.

The extent of crystallinity at different temperatures was investigated by means of a POM with crossed polarization filters and wide angle X-ray scattering (WAXS) experiments of the material T-T^{3}PPD(5)P^{4}PCL(18,50) between ambient temperature (POM) respectively 30 °C (WAXS) and 90 °C. The POM pictures showed a change in morphology between 50 °C and 60 °C correlated to the melting of the crystalline PCL domains. Comparison of the pictures taken at ambient temperature and at 66 °C exhibited a significant decrease in the extent of crystalline regions (Supporting information Fig. S3). The pattern of those regions suggests a phase-segregation into domains of high PPD content (crystalline) and domains of high PCL concentration (amorphous, black). In WAXS experiments the degree of crystallinity was

determined as 49.9 ± 0.2% at 30 °C and 24.2 ± 0.4% at 60 °C. This finding supports the assumption that in this sample with a PCL content of 50 wt% both polyester components equally contributed to the overall crystallinity. From the measurement at 90 °C a degree of crystallinity of 0% was obtained.

From the above discussed results it could be concluded that all T-T^{3}PPD(5) based copolymer networks fulfilled the requirements for triple-shape capability. Both segments crystallized independently leading to segregated crystalline phases showing two T_ms and T_cs with a sufficient temperature difference while the contribution of the segments to the overall crystallinity directly depended from the composition of the copolymer networks.

The extent of deformation is an important criterion for the applicability of the different programming methods. The values of ε_b at different temperatures are limiting the deformability. In 2SPP the samples were deformed at T_{high} and T_{mid} while 1SPP involved the deformation at T_{high} and c1SPP at ambient temperature. Therefore, the mechanical properties of the polymer networks were determined by tensile tests at ambient temperature (= 25 °C), T_{mid} = 60 °C and T_{high} = 100 °C. The determined values for the elasticity modulus (E), tensile strength (σ_b) and ε_b are summarized in **Tab. 2**.

Typical stress-strain curves are exemplarily shown in supporting information Figure S4. At 25 and 60 °C the curves are characterized by a rapid increase in stress during stretching over a wide range (above 50% strain). This indicates strain-induced crystallization (SIC)[27], which is more pronounced at 25 °C where both segments contribute to SIC resulting from the disentanglement, alignment, and crystallization of the polymer chain segments of the amorphous regions. SIC is an important process in shape-fixation during c1SPP.

Insert Table 2 here.

The stress-strain curves at 25 °C generally showed a yield point, attributed to the end of crystalline domains alignment in the amorphous matrix and the begin of plastic deformation of the crystalline domains by reorganization of the folded chain crystallites to extended chain crystallites in the direction of the applied stress. Macroscopically, this yield point could be observed with the beginning of samples' necking, which ceased at elongations between 200% and 300% and did not occur at higher temperatures. The elasticity at 25 °C of the copolymer networks was dominated by μ_{PCL} and decreased with decreasing μ_{PCL} as well as increasing PCL chain length. However, ε_b was not affected by this decrease in elasticity. All copolymer networks showed values of ε_b at 25 °C between 490 and 760%, which was significantly higher than ε_b of the homopolymer networks. The decrease in crosslink density by incorporation of three arm PPD precursors resulted in a higher mobility of the polymer chain segments and thus in an increase of ε_b of the copolymer networks. This finding indicates that both polymer segments were deformed during cold stretching of the copolymer networks.

At 60 °C the crystalline PCL domains were molten and *E* decreased by about one order of magnitude compared to 25 °C. The ε_b of the copolymer networks decreased slightly having values between 150 and 620%, which is sufficient for the second programming step of 2SPP. It could be observed that ε_b of the homopolymer networks T-T^{3}PPD(5) and T-P^{4}PCL(18) did not decrease significantly from 25 °C to 60 °C, which was attributed to the low crosslink density of these polymer networks due to the three arm precursor respectively the highest chain segment length compared to all homopolymer networks.

At 100 °C no crystalline domains remain and *E* further decreased except for the PCL homopolymer networks, which were already completely amorphous at 60 °C. All copolymer networks exhibited values of ε_b at 100 °C between 100 and 250% (exception T-T^{3}PPD(5)P^{4}PCL(5,75) with ε_b = 70%), which enables the application of 1SPP. In order to

create TSE both polymer segments have to be oriented during deformation. Therefore a high elongation close to ε_b is necessary.

All investigated copolymer networks showed mechanical properties at T_{mid} and T_{high}, which enable the application of 2SPP and 1SPP as programming procedures of TSE. A programming elongation of at least 100% at T_{high} was desired to create triple-shape capability. Only three copolymer networks had to be programmed with a lower programming elongation. The exceptional high values of ε_b at ambient temperature enabled c1SPP for all copolymer networks.

2.1. Triple-shape effect created by application of 2SPP

2SPP comprises two steps starting with an elongation of 50% at T_{high} followed by a second deformation at T_{mid} of additional 50% resulting in a total elongation of 100%. The influence of M_n and content of the PCL precursors in the copolymer networks on the TSE was investigated:

- on the separation of the two recovery steps,
- on the contribution of the recovery steps relative to the overall recovery, and
- on the T_{sw}s.

In the cooling process of 2SPP during cooling from T_{high} to T_{mid} under constant stress most samples contracted and started to slowly elongate again as soon as T_{mid} was reached (**Fig. 3A**). A substantial contraction during cooling under constant stress was obtained from P^4PCL(20) based copolymer networks and was attributed to PCL domains forming folded chain crystallites. The effect of elongation under constant stress at T_{mid} was most pronounced for the copolymer networks containing P^4PCL(5) reaching 95% of ε^0_B and was attributed to crystallization-induced elongation due to slow crystallization of the pre-oriented PPD polymer chain segments in load direction.[23, 24] However, crystallization-induced elongation was more

or less compensated by elastic contraction during unloading, which resulted from the remaining amorphous part of PCL domains at T_{mid}. The period of constant stress at T_{mid} was extended to 120 min to achieve equilibrated sample strain.

The determined average values for the shape fixity ratio (R_f) of both temporary shapes, the ratio of shape recovery (R_r) of shape (B) and shape (C) as well as the switching temperatures (T_{sw}) of those copolymer networks showing TSE are listed in **Tab. 3**. Shapes $\varepsilon_C(1)$ and $\varepsilon_C(2)$ differed substantially, so that the first cycle was used as a training cycle and was not used for the quantification of R_r and R_f. T_{sw}s did not show a discrepancy between cycles 1 and 2. Here, cycles 1 to 5 were used for quantification of T_{sw}. The fixation of shape (B) reached values of $R_f(C\rightarrow B)$ over 90% only for networks with $\mu_{PCL} = 25\%$. At T_{mid} the deformation was less effectively fixed by PPD crystallites with decreasing PPD content of the copolymer network. $R_f(C\rightarrow B)$ was also decreasing with decreasing M_n of the PCL precursor and no fixation of shape (B) could be obtained in the copolymer network T-T^{3}PPD(5)P^{4}PCL(5,75). These findings reflect the behavior of the $T_{c,PPD}$ in the copolymer networks, which was decreasing with M_n of the PCL precursors and increasing μ_{PCL}. The fixation of shape (A) being attributed to the PCL crystallization reached values of $R_f(B\rightarrow A)$ between 82% and 99%, which was increasing with increasing PCL content. The recovery of shape (B) did not reflect the observation of the shape fixation with values of $R_r(A\rightarrow B)$ between 56% and 88%, which leads to the conclusion that at T_{mid} the PPD domains were substantially deformed by cold drawing thus contributing to the second deformation step during 2SPP.

The influence of M_n of the PCL precursors and μ_{PCL} on TSE could be observed on the shifting ratio of the two recovery steps relative to the overall recovery. The ratio of the first recovery step $\Delta_{rel}\varepsilon(A\rightarrow B)$ decreased with decreasing PCL chain segment length in favor of the PPD related recovery $\Delta_{rel}\varepsilon(B\rightarrow C)$ (**Fig. 3B**). The shorter the PCL chain segments the lower was the extent of PCL deformation in favor of PPD deformation during 2SPP.

Furthermore, within the series of P^4PCL(10) and P^4PCL(5) based copolymer networks $\Delta_{rel}\varepsilon$(A→B) was decreasing with decreasing μ_{PCL}, supporting the assumption of cold-drawing of the PPD polymer chain segments during the second step of 2SPP (**Fig. 3C**). The copolymer networks T-T^3PPD(5)P^4PCL(5,y) having μ_{PCL} between 25% and 50 wt% showed no TSE. The PCL related recovery step was too small to be evaluated, which led to the conclusion that short PCL chain segments combined with a low μ_{PCL} resulted in a poor contribution of the PCL segment to the deformation during 2SPP.

T_{sw}s were generally slightly higher than T_ms but showed the same dependence from M_n of the PCL precursors exhibiting decreased values with decreased M_n of the incorporated PCL precursors. In the T-T^3PPD(5)P^4PCL(10,y) and the T-T^3PPD(5)P^4PCL(5,y) copolymer network series an influence of the PCL content on T_{sw} could be observed (Fig. 3C). Both T_{sw}s were increasing with decreasing PCL content, which was attributed to a better crystallization during programming due to the decreasing crosslink density with decreasing PCL-content. This tendency was not observed for the position of the T_ms of these copolymer network series in DSC measurements.

Insert Figure 3 here.

Insert Table 3 here.

Copolymer networks based on P^4PCL(10) with a PCL content in the range of 40 wt% to 60 wt% and copolymer networks from P^4PCL(10) and P^4PCL(5) precursors having μ_{PCL} between 50 wt% and 75 wt% exhibited good triple-shape capability with a clear separation of the two recovery steps. Moderate triple-shape properties were obtained for the copolymer networks containing P^4PCL(10) and less than 50 wt% of P^4PCL(5). Thus, it was

advantageous for copolymer networks to have a PCL content of 50 wt% or higher and longer PCL chain segments than PPD chain segments.

2.2. Triple-shape effect created by application of 1SPP

1SPP comprises the deformation of the polymer network in one step at T_{high}. all copolymer networks showing a TSE after 2SPP were investigated with the programming method 1SPP. We explored whether two well-separated thermally-induced shape-changes can be obtained under variation of the polymer chain segment lengths and the PCL content.

TSE after 1SPP requires that both polymer segments are oriented during deformation of the copolymer network and therefore was expected to depend on the elongation applied in the programming step (ε^0_A). Therefore, the influence of ε^0_A on TSE after 1SPP was investigated by variation of ε^0_A (50%, 100% and 150%) on the copolymer network with the highest elasticity at T_{high} (**Fig. 4A**). The relation of the two recovery steps shifted with $\Delta_{rel}\varepsilon(A\rightarrow B)$ increasing from 26% to 47 % while $\Delta_{rel}\varepsilon(B\rightarrow C)$ being related to the PPD segment was decreasing accordingly. This behavior can be explained by a primary deformation of the PPD segment followed by the deformation of the PCL segment, which increased with higher values of ε^0_A. Therefore, values for ε^0_A between 60% and 80% of ε_b(100 °C) were chosen for each copolymer network to deform both polymer segments sufficiently.

A substantial CIE during cooling was observed for most copolymer networks, which contributed to the overall elongation and was caused by both segments[24] increasing the samples elongation by 23% to 92%. This effect was more pronounced with increasing value of ε^0_A being attributed to the higher extent of orientation of the polymer chains of both segments. Copolymer networks from the different series having the same PCL content showed a more pronounced CIE with decreasing M_n of the PCL precursor when the same ε^0_A of 100% was applied (**Fig. 4B**).

The results obtained from recovery experiments (heating to T_{high} under stress-free conditions) after 1SPP are shown in Figure 4, the determined average values for R_f(C→A), R_r(A→C), $\Delta_{rel}\varepsilon$ for both recovery steps, and the T_{sw}s of copolymer networks showing TSE after 1SPP are listed in **Tab. 4**. Eight copolymer networks showed a TSE after application of 1SPP. In the investigated copolymer networks as in the MACL system the segments were connected on both ends to the network crosslinks.[12]

Insert Figure 4 here.

A PCL content of at least 50 wt% was necessary to obtain TSE after 1SPP supporting the assumption that PPD chain segments were primarily oriented during deformation at T_{high}. However, it has to be pointed out that the limited ε^0_A that could be applied to some copolymer networks could also have a diminishing effect on PCL deformation. The relative ratios of the two recovery steps remained constant with varying M_n of the PCL precursors and depended only from μ_{PCL} and ε^0_A. $T_{sw,PCL}$ decreased with decreasing PCL chain length, which resulted from the influence of M_n of the PCL precursors on $T_{m,PCL}$.

Insert Table 4 here.

2.3. Triple-shape effect created by application of c1SPP

c1SPP comprises the deformation of the polymer network in one step at ambient temperature. The realization of a TSE after 1SPP and the high values of ε_b determined in tensile tests at ambient temperature of the copolymer networks led to the assumption that TSE after c1SPP could potentially be achieved. It was investigated whether both polymer segments

can be oriented and fixed in a way that enables triple-shape capability depending on M_n and content of the PCL precursors.

A value of 300% was selected for ε^0_A to overcome necking shown in tensile tests at 25 °C and thus ensure shape-fixation taking place all over the sample. Five copolymer networks were chosen for cold drawing experiments including candidates from all copolymer network series to study function-property relationships. From each series the copolymer network with μ_{PCL} = 50 wt% was chosen since this composition showed good results in creation of a TSE after 1SPP. The P^4PCL(18) based series contained copolymer networks showing a pronounced TSE after 2SPP over the entire range of μ_{PCL} so that three copolymer networks from this series with μ_{PCL} = 75, 50 and 25 wt% were chosen to investigate the influence of μ_{PCL} on TSE after c1SPP. Typical recovery curves are shown in **Fig. 5**.

Insert Figure 5 here.

The average values for R_f(C→A), R_r(A→C), $\Delta_{rel}\varepsilon$ for both recovery steps, and the T_{sw}s determined from shape recovery experiments under stress-free conditions are listed in Table 4. Since the copolymer networks were highly elastic at ambient temperature the shape fixation was lower than 80%. The remaining elongation after unloading (ε_A) is also given in Table 4.

Copolymer networks showed an increased elastic contraction after unloading with decreasing PCL chain segment lengths, which can be explained by the lower extent of entanglement of the shorter chain segments that can be translated into oriented reorganization during elongation. During heating a significant decrease in elongation was observed between ambient temperature and the expected $T_{m,PCL}$ leading to an indistinct start of the first recovery step, which was attributed to an elastic contraction due to increasing elasticity during heating and the melting of imperfect and small crystallites having low T_ms, which were formed during

strain-induced crystallization. In four of the selected copolymer networks for the first time a TSE after cold stretching could be successfully demonstrated.

A systematic shift of the relative ratio of the two recovery steps depending on the PCL chain length was not observed (Figure 5A). All copolymer networks showed the first recovery step more pronounced than the second recovery step. The reason behind this PCL-dominated shape fixation could be an asymmetric distribution of the applied deformation at ambient temperature with the PCL segments respectively domains being deformed to a higher extend than the PPD segments respectively domains and/or unequal distribution of the elastic contraction after unloading between the PCL and PDL domains. The first explanation is supported by the significantly lower *E* moduli at ambient temperature of the T-P^{4}PCL homopolymer networks compared to the *E* modulus of the T-T^{3}PDL homopolymer network (Table. 2). The copolymer network T-T^{3}PPD(5)P^{4}PCL(18,25) exhibited no triple-shape capability (Figure 5B). This result means that a small PCL content of 25 wt% is not sufficient to obtain a distinct PCL related recovery step, although the shape recovery slowly proceeded to about half of the elongation until the PPD related T_{sw} was reached. As already observed after 2SPP the switching temperature $T_{sw,PCL}$ decreased with decreasing PCL chain segment length. The determined values for T_{sw} were comparable with those from the experiments applying 2SPP and 1SPP.

Copolymer networks showing TSE after c1SPP had a PCL content between 50 and 75 wt%, which was already found to be favorable for the TSE after 1SPP. However, a fixed elongation of more than 200% could not be achieved at T_{high} being limited by lower values of ε_b of the copolymer networks at this temperature. Limitations in the elasticity at T_{high} could be avoided by applying a c1SPP at ambient temperature. The c1SPP further simplifies the programming process of the triple-shape effect and enables the realization of one-step deformations of a much higher extent.

3. Conclusion

A triple-shape capability could be obtained by application of 2SPP for almost all copolymer networks based on the T^{3}PPD(5) precursor. The application of PCL precursors with $M_n > 5000$ g·mol^{-1} and a PCL content $\mu_{PCL} > 25$ wt% were favorable. Most of these copolymer networks exhibited TSE after 1SPP, whereas the PCL content had to be at least 50 wt%.

Selected copolymer networks, representing all copolymer series and three different compositions within one copolymer series were investigated by applying c1SPP. A TSE with two separated recovery steps after c1SPP required a PCL content of at least 50 wt%. In four copolymer networks the TSE could be generated by c1SPP, which simplifies the programming procedure considerably by reducing the time for the programming process substantially since no heating was necessary. But more important, this novel gentle triple-shape creation procedure by programming at ambient temperature enables the triple-shape capability of polymer systems, which have poor mechanical properties at T_{high} but can be deformed by cold drawing. In this way the triple-shape technology is greatly improved. Furthermore, a possible thermal degradation occurring during programming can be avoided. The versatility of this copolymer system makes it an interesting candidate for applications in fixation systems or disassembling systems. A structuring of such copolymer networks on the microlevel could enable adhesives with temperature dependent adhesion rates or thermally controlled reversible adhesive systems.[28, 29] Furthermore, the versatile copolymer network could form the basis for a multifunctional material system,[30, 31] in which additional functions could be introduced such as a twofold change of color when shapes (B) and (C) are recovered.[32]

4. Experimental

Materials: Mixture of 2-ethyl-2-(hydroxymethyl)propane-1,3-diol 6-hydroxycaproates (T^3, $M_n \approx 300$ g·mol^{-1}), pentaerythritol (P^4), DBTDL (all Sigma-Aldrich, Munich, Germany), 15-pentadecalactone (PDL, Macrolid Supra, Th. Geyer, Friedrichsthal, Germany), ε-caprolactone (CL) and DBTO (Fluka, Taufkirchen, Germany), CAPA4801 (P^4PCL(10), Solvay, Warringthon, UK) were used as received. TMDI (Sigma-Aldrich) was distilled in vacuum prior to reaction.

Polymer network preparation: The star-shaped precursors were synthesized from the cyclic monomers in bulk under nitrogen atmosphere at 130° C catalyzed by DBTO and purified by precipitation of a dichloromethane solution in cold hexane. The synthesis of the polymer networks was performed in dichloroethane solution under nitrogen atmosphere by reacting the star-shaped hydroxytelechelic precursors with TMDI using DBTDL as catalyst [19, 24]. Quantities of the reactants are summarized in supporting information Table S2.

Characterization methods: OH-numbers of the precursors were determined with the titrator system 716 DMS/719 S Titrino and a combined LiCl-electrode (Metrohm, Filderstadt, Germany).

The GPC measurements, DSC measurements, WAXS measurements, and tensile tests were performed as stated reference [24]. DMTA measurements were conducted on a Gabo (Ahlden, Germany) Eplexor® 25 N in temperature sweep mode with a constant heating rate of 2 K·min^{-1} and an oscillation frequency of 10 Hz in the temperature range from -100 °C to 100 °C.

For investigations in cyclic thermomechanical measurements polymer films were cut into standard samples (ISO 527–2/1BB) and strained at an elongation rate of 10 mm·min^{-1}. In 2SPP the sample was stretched at T_{high} (100 °C) from ε_C to $\varepsilon^0_B = 50\%$ and equilibrated for 5 min. The sample was cooled with a cooling rate of 5 K·min^{-1} to T_{mid} (60 °C) under stress-

control and unloaded after 120 min. The sample was then further stretched to the maximum programmed elongation (ε^0_A, 100%), equilibrated for 5 min and cooled to T_{low} (0 °C) under stress-control with a cooling rate of 5 K·min^{-1}. Shape (A) was obtained by unloading after 10 min. The recovery process of the sample was monitored by reheating with a heating rate of 1 K·min^{-1} from T_{low} to T_{high} while the stress is kept at 0 MPa. Shape (B) was characterized by ε_{ip}, which is defined as the elongation at the inflection point where the recovery rate has a minimum. The T_{sw}s representing the temperatures at the maximum shape recovery rates were determined at maximal absolute values of $\Delta\varepsilon/\Delta T$ during the recovery process. The strain fixity ratios R_f and strain recovery ratios R_r were determined using the following equations (N is the cycle number):

$$R_f(X \rightarrow Y) = \frac{\varepsilon_Y(N) - \varepsilon_X(N-1)}{\varepsilon_{Yload}(N) - \varepsilon_X(N-1)} \quad (1)$$

$$R_r(A \rightarrow B) = \frac{\varepsilon_A(N) - \varepsilon_{ip}(N)}{\varepsilon_A(N) - \varepsilon_B(N)} \quad (2)$$

$$R_r(A \rightarrow C) = \frac{\varepsilon_A(N) - \varepsilon_C(N)}{\varepsilon_A(N) - \varepsilon_C(N-1)} \quad (3)$$

In 1SPP the sample was stretched at T_{high} from ε_C to ε^0_A, equilibrated for 5 min and cooled to T_{low} under stress-control with a cooling rate of 5 K·min^{-1}, whereas the elongation changed to ε_{Aload} and after 10 min unloading led to ε_A. The recovery process of the sample was conducted as described after 2SPP. The strain fixity ratio R_f(C→A) was calculated according to equation (1) and the strain recovery ratio R_r(A→C) was determined using equation (3).

In c1SPP the sample was stretched at T_{low} from ε_C to ε^0_A and equilibrated for 5 min. Unloading led to ε_A. The recovery process of the sample was conducted as described after 2SPP. The strain fixity ratio R_f(C→A) and the strain recovery ratio R_r(A→C) were determined according to equations (1) and (3). All cyclic thermo-mechanical measurements were conducted five times. The ratio of a single recovery step relative to the overall recovery

$\Delta_{rel}\varepsilon(A\rightarrow B)$ and $\Delta_{rel}\varepsilon$ $(B\rightarrow C)$ in all recovery experiments were calculated according to equation (4), whereas ε_B was always replaced by ε_{ip}:

$$\Delta_{rel}\varepsilon(X\rightarrow Y) = (\varepsilon_X - \varepsilon_Y)/(\varepsilon_A - \varepsilon_C) \quad (4)$$

The method of taking morphology pictures on a polarizing optical microscope is described in supporting information method S5.

References:

[1] M. Behl, A. Lendlein, *Soft Matter* **2007**, *3*, 58.
[2] M. Behl, J. Zotzmann, A. Lendlein, *"Shape-Memory Polymers and Shape-Changing Polymers"*, in: *"Advances in Polymer Science"*, Springer, Berlin / Heidelberg **2009**, p. E-pub ahead of print on November 5th 2009, DOI: 2010.1007/2012_2009_2026.
[3] P. T. Mather, X. F. Luo, I. A. Rousseau, *Annu. Rev. Mater. Res.* **2009**, *39*, 445.
[4] N. Y. Choi, S. Kelch, A. Lendlein, *Adv. Eng. Mater.* **2006**, *8*, 439.
[5] N. Y. Choi, A. Lendlein, *Soft Matter* **2007**, *3*, 901.
[6] S. Kelch, N. Y. Choi, Z. Wang, A. Lendlein, *Adv. Eng. Mater.* **2008**, *10*, 494.
[7] S. Kelch, S. Steuer, A. M. Schmidt, A. Lendlein, *Biomacromolecules* **2007**, *8*, 1018.
[8] I. Bellin, S. Kelch, R. Langer, A. Lendlein, *Proc. Natl. Acad. Sci. U.S.A.* **2006**, *103*, 18043.
[9] I. S. Kolesov, H.-J. Radusch, *Expr. Polym. Lett.* **2008**, *2*, 461.
[10] M. Behl, A. Lendlein, *J. Mater. Chem.* **2010**, DOI: 10.1039/B922992B.
[11] T. Xie, X. Xiao, Y.-T. Cheng, *Macromol. Rapid Commun.* **2009**, *30*, 1823.
[12] I. Bellin, S. Kelch, A. Lendlein, *J. Mater. Chem.* **2007**, *17*, 2885.
[13] W. Wagermaier, T. Zander, D. Hofmann, K. Kratz, U. N. Kumar, A. Lendlein, *Macromol. Rapid Commun.* **2010**, submitted.
[14] T. Pretsch, *Smart Mater. Struct.* **2010**, *19*, 015006.
[15] T. Xie, *Nature* **2010**, *464*, 267.
[16] M. Behl, I. Bellin, S. Kelch, W. Wagermaier, A. Lendlein, *Adv. Funct. Mater.* **2009**, *19*, 102.
[17] K. Kratz, U. Voigt, W. Wagermaier, A. Lendlein. in *MRS Spring Meeting* **2009**. San Francisco, *1140*, p. 17-22.
[18] R. Mohr, K. Kratz, T. Weigel, M. Lucka-Gabor, M. Moneke, A. Lendlein, *Proc. Natl. Acad. Sci. USA* **2006**, *103*, 3540.
[19] A. Alteheld, Y. Feng, S. Kelch, A. Lendlein, *Angew. Chem. Int. Ed.* **2005**, *44*, 1188.
[20] C. P. Buckley, C. Prisacariu, A. Caraculacu, *Polymer* **2007**, *48*, 1388.
[21] A. Lendlein, J. Zotzmann, Y. Feng, A. Alteheld, S. Kelch, *Biomacromolecules* **2009**, *10*, 975.
[22] L. Xue, S. Dai, Z. Li, *Macromolecules* **2009**, *42*, 964.
[23] T. Chung, A. Romo-Uribe, P. T. Mather, *Macromolecules* **2008**, *41*, 184.
[24] J. Zotzmann, M. Behl, D. Hofmann, A. Lendlein, *Adv. Mater.* **2010**, *published online on 04/19/2010*, DOI: 10.1002/adma.200904202.
[25] J. Zotzmann, A. Alteheld, M. Behl, A. Lendlein, *J. Mater. Sci. Mater. Med.* **2009**, *20*, 1815.

[26] M. L. Focarete, M. Scandola, A. Kumar, R. A. Gross, *J. Polym. Sci. B Polym. Phys.* **2001**, *39*, 1721.
[27] P. J. Flory, *J. Chem. Phys.* **1947**, *15*, 397.
[28] S. Reddy, E. Arzt, A. del Campo, *Adv. Mater.* **2007**, *19*, 3833.
[29] T. Xie, X. Xiao, *Chem. Mater.* **2008**, *20*, 2866.
[30] M. Behl, M. Y. Razzaq, A. Lendlein, *Adv. Mater.* **2010**, *published online*, DOI: 10.1002/adma.200904447.
[31] A. Lendlein, S. Kelch, *Mater. Sci. Forum* **2005**, *492-493*, 219.
[32] J. Kunzelman, T. Chung, P. T. Mather, C. Weder, *J. Mater. Chem.* **2008**, *18*, 1082.

Figures:

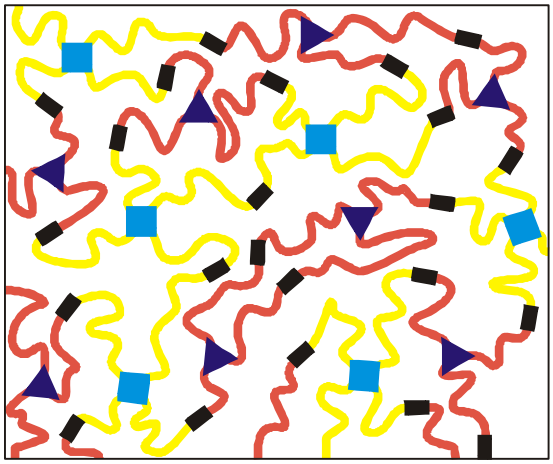

Figure 1. Schematic architecture of the PPD/PCL-copolymer networks; ▲: three arm net point; ■: four arm net point; ▬: PPD chain segment; ▬: PCL chain segment; ▬: diurethane linker.

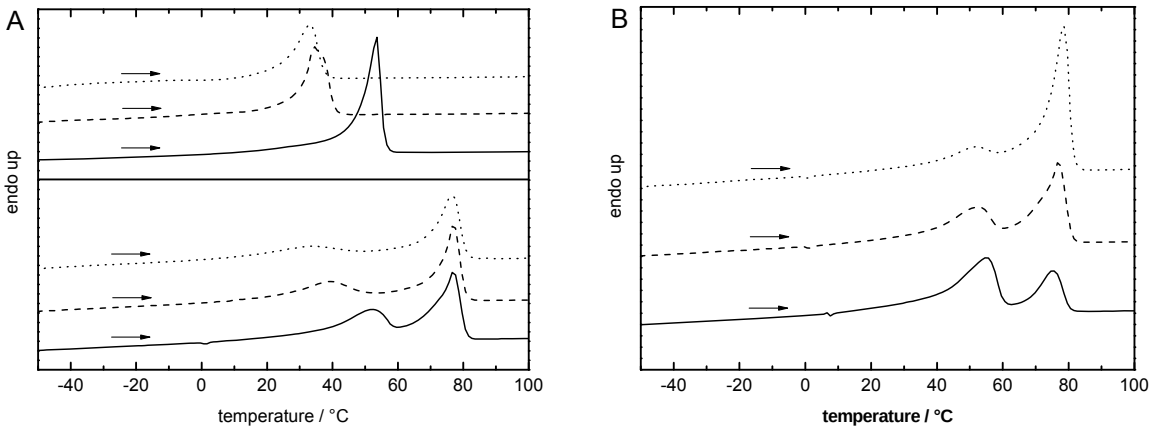

Figure 2. Comparison of DSC thermograms of 2nd heating runs; A top: homopolymer networks, solid line T-P^4PCL(18), dashed line: T-P^4PCL(10), dotted line: T-P^4PCL(5), bottom: copolymer networks with a PCL-content of 50 wt%, solid line: T-T^3PPD(5)P^4PCL(18,50), dashed line: T-T^3PPD(5)P^4PCL(10,50), dotted line: T-T^3PPD(5)P^4PCL(5,50); B: copolymer networks containing P^4PCL(18) precursors; solid line: T-T^3PPD(5)P^4PCL(18,75), dashed line: T-T^3PPD(5)P^4PCL(18,50), dotted line: T-T^3PPD(5)P^4PCL(18,25).

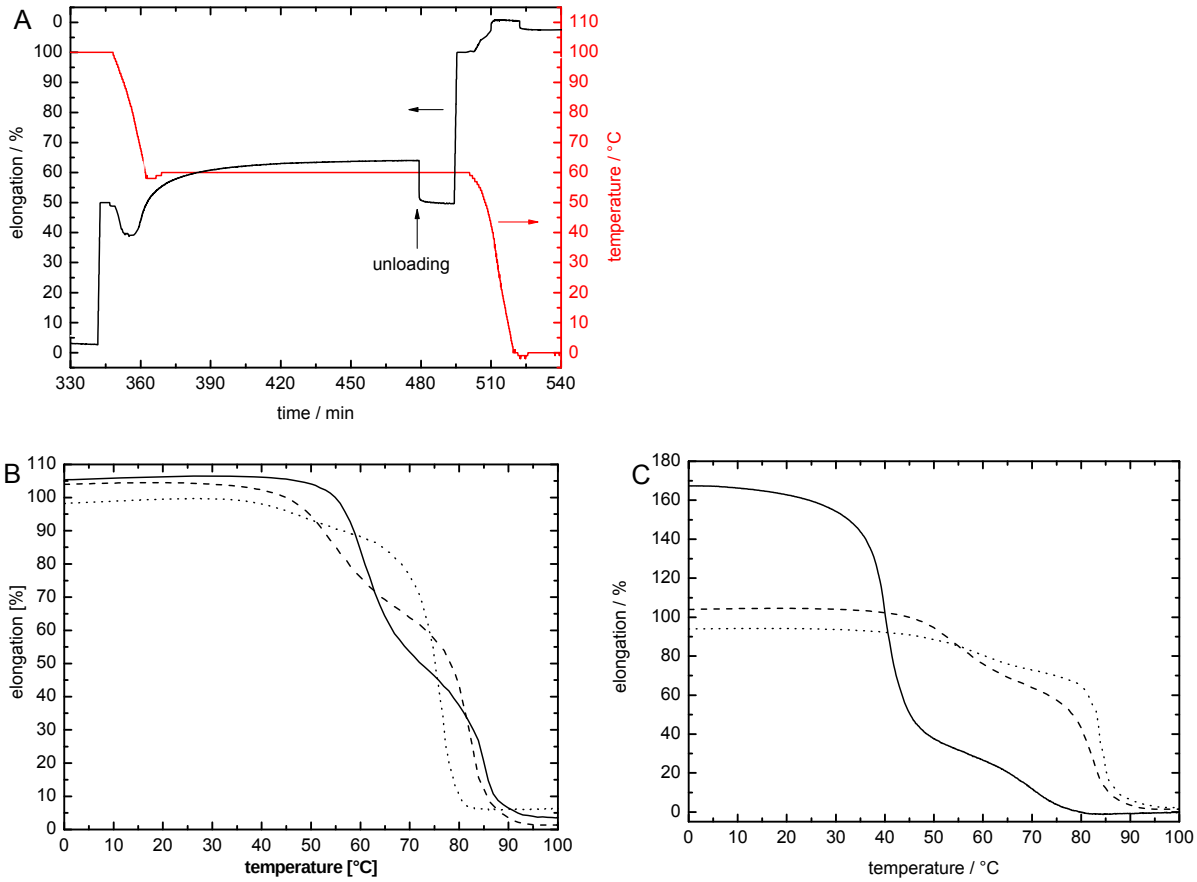

Figure 3. Cyclic, thermomechanical experiments (2nd cycle) under stress-control; applying 2SPP with T_{high} = 100 °C, T_{mid} = 60 °C, T_{low} = 0 °C, ε^0_B = 50%, ε^0_A = 100%, a cooling rate of 5 K·min^{-1}, and a heating rate of 1 K·min^{-1}; A: elongation/time curve of 2SPP of copolymer networks, black line: T-T^{3}PPD(5)P^{4}PCL(5,50), red line: temperature; B: comparison of shape recovery curves of copolymer networks with a PCL-content of 50 wt%, solid line: T-T^{3}PPD(5)P^{4}PCL(18,50), dashed line: T-T^{3}PPD(5)P^{4}PCL(10,50), dotted line: T-T^{3}PPD(5)P^{4}PCL(5,50); C: comparison of shape recovery curves of copolymer networks based on P^{4}PCL(10) precursors; solid line: T-T^{3}PPD(5)P^{4}PCL(10,75), dashed line: T-T^{3}PPD(5)P^{4}PCL(10,50), dotted line: T-T^{3}PPD(5)P^{4}PCL(10,25).

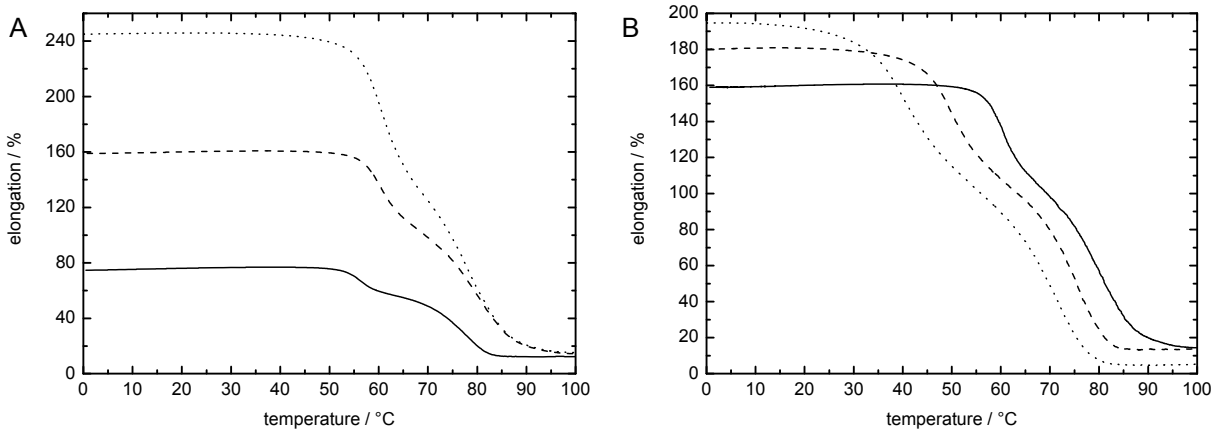

Figure 4. Comparison of, recovery after application of 1SPP (2nd cycle) under stress control determining in cyclic, thermo-mechanical experiments ; A: T-T^{3}PPD(5)P^{4}PCL(18,60), solid line: ε^0_A = 50%, dashed line: ε^0_A = 100%, dotted line: ε^0_A = 150%; B: ε^0_A = 100%, solid line: T-T^{3}PPD(5)P^{4}PCL(18,60), dashed line: T-T^{3}PPD(5)P^{4}PCL(10,60), dotted line: T-T^{3}PPD(5)P^{4}PCL(5,60).

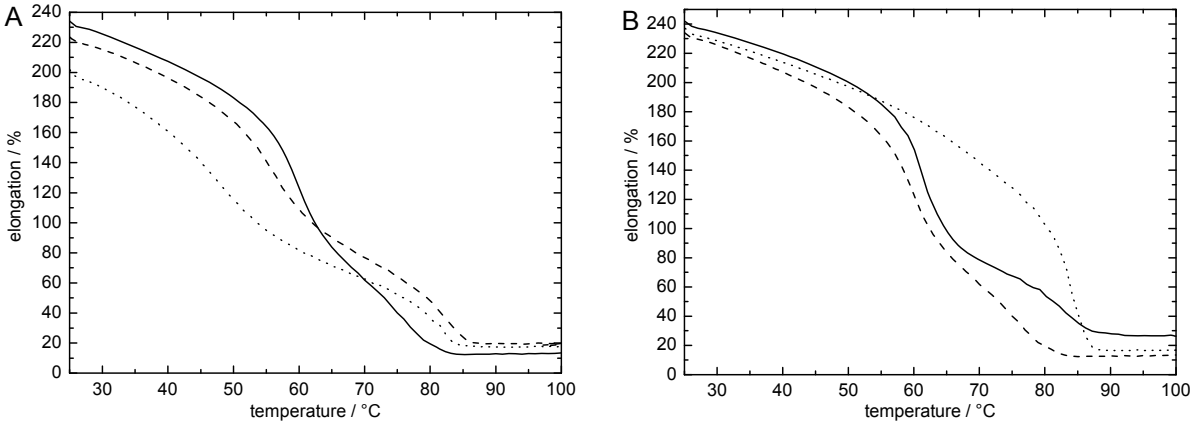

Figure 5. Comparison of typical shape recovery curves from cyclic, thermomechanical experiments (2nd cycle) under stress-control after c1SPP; A: copolymer networks with a PCL-content of 50 wt%, solid line: T-T^{3}PPD(5)P^{4}PCL(18,50), dashed line: T-T^{3}PPD(5)P^{4}PCL(10,50), dotted line: T-T^{3}PPD(5)P^{4}PCL(5,50); B: copolymer networks containing P^{4}PCL(18); solid line: T-T^{3}PPD(5)P^{4}PCL(18,75), dashed line: T-T^{3}PPD(5)P^{4}PCL(18,50), dotted line: T-T^{3}PPD(5)P^{4}PCL(18,25).

Tables

Table 1. Thermal properties of the polymer networks determined by DSC measurements.

Sample ID[a]	T_g [°C]	$T_{m,PCL}$ [°C]	$T_{m,PPD}$ [°C]	$\Delta_m H_1$[b] [J·g^{-1}]	$\Delta_m H_{PCL}$[c] [J·g^{-1}]	$\Delta_m H_2$[b] [J·g^{-1}]	$\Delta_m H_{PPD}$[c] [J·g^{-1}]	$T_{c,PCL}$ [°C]	$T_{c,PPD}$ [°C]	$\Delta_c H_1$[b] [J·g^{-1}]	$\Delta_c H_{PCL}$[c] [J·g^{-1}]	$\Delta_c H_2$[b] [J·g^{-1}]	$\Delta_c H_{PPD}$[c] [J·g^{-1}]
T-P^{4}PCL(18)	-60	53	--	60	60	--	--	23	--	-55	-55	--	--
T-P^{4}PCL(10)	-54	34	--	41	41	--	--	0	--	-48	-48	--	--
T-P^{4}PCL(5)	-44	32	--	36	36	--	--	-12	--	-39	-39	--	--
T-T^{3}PPD(5)P^{4}PCL(18,75)	--	55	75	56	75	21	82	32	--	-73	-73	--	--
T-T^{3}PPD(5)P^{4}PCL(18,60)	--	54	77	41	68	31	77	37	46	-49	-82	-25	-61
T-T^{3}PPD(5)P^{4}PCL(18,50)	--	53	77	29	59	40	80	31	60	-45	-91	-34	-67
T-T^{3}PPD(5)P^{4}PCL(18,40)	--	54	79	33	82	53	89	37	61	-35	-88	-50	-83
T-T^{3}PPD(5)P^{4}PCL(18,25)	--	52	79	19	75	64	85	35	60	-28	-110	-66	-88
T-T^{3}PPD(5)P^{4}PCL(10,75)	-54	35	70/79[d]	35	47	21	84	20	29/64[d]	-33	-45	-22	-88
T-T^{3}PPD(5)P^{4}PCL(10,60)	-55	42	79	36	60	38	96	24	59	-40	-68	-34	-85
T-T^{3}PPD(5)P^{4}PCL(10,50)	--	40	78	30	61	44	88	29	57	-33	-66	-37	-75
T-T^{3}PPD(5)P^{4}PCL(10,40)	--	42	79	25	64	52	87	30	61	-30	-76	-49	-82
T-T^{3}PPD(5)P^{4}PCL(10,25)	--	43	79	18	70	71	95	30	62	-14	-56	-61	-81
T-T^{3}PPD(5)P^{4}PCL(5,75)	-48	31	72	34	45	19	77	17	30	-27	-36	-26	-102
T-T^{3}PPD(5)P^{4}PCL(5,60)	--	35	77	34	56	35	87	29	55	-32	-54	-31	-77
T-T^{3}PPD(5)P^{4}PCL(5,50)	--	33	75	24	48	46	92	24	54	-25	-49	-44	-88
T-T^{3}PPD(5)P^{4}PCL(5,40)	--	32	75	18	45	57	96	26	56	-21	-51	-54	-90
T-T^{3}PPD(5)P^{4}PCL(5,25)	--	--	79	--	--	66	89	--	61	--	--	-59	-79
T-T^{3}PPD(5)	--	--	81	--	--	103	103	--	63	--	--	-105	-105
T-T^{3}PPD(3)P^{4}PCL(18,75)	-57	56	72	54	72	15	60	27	48	-67	-89	- 8	-32
T-T^{3}PPD(3)P^{4}PCL(18,60)	-53	54	67	50	84	23	57	30	--	-79	-132	--	--
T-T^{3}PPD(3)P^{4}PCL(18,50)	--	54	73	41	81	37	74	33	52	-43	-86	-35	-70

T-T^{3}PPD(3)P^{4}PCL(18,40)	--	55	73	31	78	35	58	26	45	-34	-84	-38	-64
T-T^{3}PPD(3)P^{4}PCL(18,25)	--	54	75	30	121	53	71	27	49	-24	-96	-59	-78
T-T^{3}PPD(3)P^{4}PCL(10,75)	-52	35	65	42	56	17	66	13	24/51[d]	-41	-54	-17	-68
T-T^{3}PPD(3)P^{4}PCL(10,60)	-52	34	67	34	56	24	59	15	26/44[d]	-30	-50	-30	-74
T-T^{3}PPD(3)P^{4}PCL(10,50)	--	33	62/75[d]	29	57	39	79	10	24/53[d]	-28	-56	-44	-88
T-T^{3}PPD(3)P^{4}PCL(10,40)	--	40	72	29	72	36	60	17	46/51[d]	-38	-95	-33	-54
T-T^{3}PPD(3)P^{4}PCL(10,25)	--	33	73	15	59	60	80	--	54	--	--	-73	-97
T-T^{3}PPD(3)P^{4}PCL(5,75)	-44	30	63	37	50	16	66	10	24	-33	-44	-25	-100
T-T^{3}PPD(3)P^{4}PCL(5,60)	-43	25	64/72[d]	24	40	25	63	7	26/55[d]	-21	-35	-31	-76
T-T^{3}PPD(3)P^{4}PCL(5,50)	--	27	72	25	49	41	81	8	25/52[d]	-17	-33	-43	-86
T-T^{3}PPD(3)P^{4}PCL(5,40)	--	27	75	16	41	42	70	6	24/52[d]	-11	-27	-49	-81
T-T^{3}PPD(3)P^{4}PCL(5,25)	--	--	69	--	--	71	94	--	48	--	--	-69	-118
T-T^{3}PPD(3)	--	--	71	--	--	86	86	--	50	--	--	-81	-81

[a] T-T3PPD(x)P4PCL(x,y) are thermosets (T) from T3PPD segments and P4PCL segments with the approximate Mn (x·1000 g·mol^{-1}) and μ_{PCL} (y wt%) given in parenthesis, T-T^{3}PPD(x) are homopolymer network from PPD whereas T-P^{4}PCL(x) homopolymer networks contain P^{4}PCL segments only; [b] heat of melting/crystallization for the respective thermal transition; [c] partial heat of melting/crystallization for the respective component correlated to its weight fraction in the copolymer network; [d] two thermal transitions were observed, which were related to the PPD segment.

Table 2. Mechanical properties of the polymer networks at 25°C, 60°C and 100°C. The errors shown are ± standard deviation.

Sample-ID[a]	μ_{PCL}	25 °C			60 °C			100 °C		
		E	σ_b	ε_b	E	σ_b	ε_b	E	σ_b	ε_b
	[wt%]	[MPa]	[MPa]	[%]	[MPa]	[MPa]	[%]	[MPa]	[MPa]	[%]
T-P^{4}PCL(18)	100	114 ± 19	15.6 ± 1.2	420 ± 50	0.9 ± 0.1	2.0 ± 0.2	610 ± 20	0.86 ± 0.07	1.31 ± 0.09	620 ± 50
T-P^{4}PCL(10)	100	35 ± 4	7.8 ± 1.0	240 ± 10	2.9 ± 0.5	1.8 ± 0.3	140 ± 20	5.70 ± 0.31	3.22 ± 0.63	140 ± 40
T-P^{4}PCL(5)	100	19 ± 3	9.5 ± 1.5	320 ± 40	3.2 ± 0.9	1.0 ± 0.5	40 ± 20	4.36 ± 0.28	1.49 ± 0.21	40 ± 8
T-T^{3}PPD(5)P^{4}PCL(18,75)	75	273 ± 20	29.5 ± 2.3	720 ± 20	15.8 ± 1.3	4.8 ± 0.7	440 ± 30	1.84 ± 0.28	1.33 ± 0.12	170 ± 40
T-T^{3}PPD(5)P^{4}PCL(18,60)	60	332 ± 24	24.6 ± 3.9	620 ± 90	22.4 ± 3.3	6.8 ± 1.4	490 ± 40	2.16 ± 0.30	1.80 ± 0.20	250 ± 50
T-T^{3}PPD(5)P^{4}PCL(18,50)	50	319 ± 16	30.4 ± 3.5	720 ± 40	28.9 ± 2.6	6.3 ± 0.9	460 ± 20	1.88 ± 0.26	1.91 ± 0.16	200 ± 20
T-T^{3}PPD(5)P^{4}PCL(18,40)	40	272 ± 20	28.5 ± 4.7	700 ± 60	23.3 ± 4.1	12.5 ± 2.6	590 ± 50	2.08 ± 0.60	1.18 ± 0.28	120 ± 7
T-T^{3}PPD(5)P^{4}PCL(18,25)	25	300 ± 15	32.4 ± 4.2	660 ± 60	35.1 ± 3.0	8.2 ± 0.8	490 ± 20	2.36 ± 0.22	1.43 ± 0.22	150 ± 30
T-T^{3}PPD(5)P^{4}PCL(10,75)	75	101 ± 16	20.3 ± 4.0	590 ± 50	8.0 ± 0.7	5.0 ± 0.8	290 ± 50	3.75 ± 0.35	2.12 ± 0.31	130 ± 20
T-T^{3}PPD(5)P^{4}PCL(10,60)	60	185 ± 18	27.8 ± 4.3	670 ± 60	7.3 ± 1.3	6.1 ± 0.7	470 ± 30	3.25 ± 0.08	1.92 ± 0.23	160 ± 40
T-T^{3}PPD(5)P^{4}PCL(10,50)	50	207 ± 18	23.6 ± 2.6	760 ± 30	12.7 ± 2.5	7.5 ± 0.9	620 ± 20	2.41 ± 0.31	1.23 ± 0.25	100 ± 20
T-T^{3}PPD(5)P^{4}PCL(10,40)	40	257 ± 49	24.8 ± 3.5	710 ± 90	21.1 ± 6.7	6.3 ± 2.0	550 ± 40	1.97 ± 0.20	1.33 ± 0.13	210 ± 50
T-T^{3}PPD(5)P^{4}PCL(10,25)	25	340 ± 33	25.8 ± 2.5	700 ± 50	45.8 ± 8.4	9.1 ± 1.1	560 ± 60	1.79 ± 0.12	1.22 ± 0.18	230 ± 50
T-T^{3}PPD(5)P^{4}PCL(5,75)	75	73 ± 15	20.5 ± 2.0	670 ± 30	6.7 ± 0.9	2.9 ± 0.6	150 ± 40	3.38 ± 0.26	1.33 ± 0.10	70 ± 10
T-T^{3}PPD(5)P^{4}PCL(5,60)	60	179 ± 17	27.1 ± 2.5	710 ± 30	16.1 ± 5.8	3.4 ± 0.5	230 ± 40	2.98 ± 0.11	1.54 ± 0.07	100 ± 9
T-T^{3}PPD(5)P^{4}PCL(5,50)	50	131 ± 21	21.2 ± 3.4	490 ± 40	18.2 ± 3.8	4.3 ± 1.0	260 ± 40	2.53 ± 0.21	1.80 ± 0.14	210 ± 40
T-T^{3}PPD(5)P^{4}PCL(5,40)	40	154 ± 10	24.9 ± 1.9	560 ± 30	34.1 ± 7.0	7.5 ± 1.9	350 ± 40	2.23 ± 0.12	1.33 ± 0.16	160 ± 30
T-T^{3}PPD(5)P^{4}PCL(5,25)	25	274 ± 22	25.3 ± 3.9	690 ± 60	59.8 ± 6.2	8.9 ± 0.7	520 ± 40	1.47 ± 0.13	1.01 ± 0.16	190 ± 50
T-T^{3}PPD(5)	0	370 ± 87	20.9 ± 2.6	520 ± 40	102 ± 16	9.9 ± 1.2	690 ± 50	0.65 ± 0.13	1.25 ± 0.21	560 ± 70

[a] see Tab. 1 note a.

Table 3. Triple-shape properties of the copolymer networks. $\overline{R}_{f,2-5}$ *and* $\overline{R}_{r,2-5}$ are the average values for cycles 2-5. The switching temperatures $\overline{T}_{sw1,1-5}$ and $\overline{T}_{sw2,1-5}$ are average values over all 5 cycles. The errors shown are ± standard deviation.

Sample ID[a]	$\overline{R}_{f,2-5}$ (C→B)	$\overline{R}_{f,2-5}$ (B→A)	$\overline{R}_{r,2-5}$ (A→B)	$\overline{R}_{r,2-5}$ (B→C)	$\Delta_{rel}\varepsilon$ (A→B)	$\Delta_{rel}\varepsilon$ (B→C)	$\overline{T}_{sw1,1-5}$	$\overline{T}_{sw2,1-5}$
	[%]	[%]	[%]	[%]	[%]	[%]	[°C]	[°C]
T-T^{3}PPD(5)P^{4}PCL(18,75)	74.5 ± 1.0	99.0 ± 0.1	56.2 ± 1.0	96.3 ± 7.0	45 ± 3	55 ± 3	66 ± 2	85 ± 2
T-T^{3}PPD(5)P^{4}PCL(18,60)	80.1 ± 0.5	98.2 ± 0.1	81.1 ± 0.7	>99.9 ± 0.5	54 ± 1	46 ± 1	61 ± 2	84 ± 1
T-T^{3}PPD(5)P^{4}PCL(18,50)	72.5 ± 0.8	97.6 ± 0.2	80.5 ± 1.0	99.0 ± 1.0	56 ± 3	44 ± 3	61 ± 1	85 ± 1
T-T^{3}PPD(5)P^{4}PCL(18,40)	82.0 ± 1.6	96.4 ± 0.1	85.0 ± 0.7	99.4 ± 3.3	71 ± 1	29 ± 1	59 ± 1	86 ± 2
T-T^{3}PPD(5)P^{4}PCL(18,25)	91.5 ± 0.1	91.4 ± 1.0	78.8 ± 0.8	98.5 ± 2.2	48 ± 2	52 ± 2	62 ± 2	86 ± 2
T-T^{3}PPD(5)P^{4}PCL(10,75)	17.6 ± 0.9	94.2 ± 1.4	88.0 ± 2.1	99.8 ± 0.6	82 ± 2	18 ± 2	40 ± 2	70 ± 1
T-T^{3}PPD(5)P^{4}PCL(10,60)	64.2 ± 2.8	96.2 ± 0.3	88.2 ± 0.9	99.5 ± 1.0	52 ± 1	48 ± 1	48 ± 1	76 ± 1
T-T^{3}PPD(5)P^{4}PCL(10,50)	75.2 ± 0.6	95.7 ± 0.3	84.1 ± 0.7	>99.9 ± 0.5	36 ± 1	64 ± 1	55 ± 2	82 ± 1
T-T^{3}PPD(5)P^{4}PCL(10,40)	88.1 ± 0.2	91.7 ± 0.2	89.1 ± 2.1	99.8 ± 3.8	29 ± 2	71 ± 2	56 ± 2	84 ± 1
T-T^{3}PPD(5)P^{4}PCL(10,25)	93.2 ± 0.3	89.1 ± 0.2	81.5 ± 1.0	99.9 ± 2.5	24 ± 2	75 ± 2	61 ± 2	84 ± 1
T-T^{3}PPD(5)P^{4}PCL(5,75)	2.0 ± 0.9	97.7 ± 0.1	76.5 ± 0.8	99.8 ± 0.3	76 ± 1	24 ± 1	37 ± 1	69 ± 1
T-T^{3}PPD(5)P^{4}PCL(5,60)	75.5 ± 1.3	95.2 ± 0.3	81.1 ± 1.5	>99.9 ± 1.2	44 ± 1	56 ± 1	48 ± 2	82 ± 2

[a] see Table 1 note a.

Table 4. Triple-shape properties of copolymer networks after 1SPP and c1SPP. $\overline{R}_{f,2-5}$ *and* $\overline{R}_{r,2-5}$ are the average values for cycles 2-5, the switching temperatures $\overline{T}_{sw1,1-5}$ and $\overline{T}_{sw2,1-5}$ are average values over all 5 cycles. The errors shown are ± standard deviation.

	Sample ID[a]	ε^0_A [%]	ε_A [%]	$\overline{R}_{f,2-5}$ (C→A) [%]	$\overline{R}_{r,2-5}$ (A→C) [%]	$\Delta_{rel}\varepsilon$ (A→B) [%]	$\Delta_{rel}\varepsilon$ (B→C) [%]	$\overline{T}_{sw1,1-5}$ [°C]	$\overline{T}_{sw2,1-5}$ [°C]
1SPP	T-T^{3}PPD(5)P^{4}PCL(18,60)	50	73 ± 2	98.0 ± 1.3	99.9 ± 4.8	26 ± 3	74 ± 3	57 ± 1	79 ± 2
	T-T^{3}PPD(5)P^{4}PCL(18,60)	100	158 ± 4	97.2 ± 0.4	98.8 ± 0.8	37 ± 3	63 ± 3	61 ± 1	80 ± 2
	T-T^{3}PPD(5)P^{4}PCL(18,60)	150	242 ± 3	98.3 ± 0.1	99.0 ± 0.4	47 ± 3	53 ± 3	61 ± 1	79 ± 2
	T-T^{3}PPD(5)P^{4}PCL(18,50)	150	277 ± 15	98.8 ± 0.6	99.0 ± 0.4	24 ± 1	76 ± 1	58 ± 1	78 ± 1
	T-T^{3}PPD(5)P^{4}PCL(10,75)	70	160 ± 1	97.6 ± 0.1	99.8 ± 0.1	77 ± 1	23 ± 1	42 ± 1	69 ± 1
	T-T^{3}PPD(5)P^{4}PCL(10,60)	100	181 ± 3	98.2 ± 0.2	98.2 ± 0.9	46 ± 1	54 ± 1	50 ± 1	75 ± 1
	T-T^{3}PPD(5)P^{4}PCL(10,50)	80	152 ± 1	98.1 ± 0.3	99.5 ± 0.1	34 ± 1	66 ± 1	50 ± 1	76 ± 1
	T-T^{3}PPD(5)P^{4}PCL(5,75)	50	113 ± 1	97.4 ± 0.1	99.3 ± 0.1	72 ± 1	28 ± 1	36 ±1	66 ± 1
	T-T^{3}PPD(5)P^{4}PCL(5,60)	100	196 ± 1	97.5 ± 0.1	99.3 ± 0.2	49 ± 1	51 ± 1	40 ±1	71 ± 2
	T-T^{3}PPD(5)P^{4}PCL(5,50)	100	177 ± 2	95.8 ± 0.3	99.3 ± 0.2	26 ± 1	74 ± 1	46 ± 2	78 ± 1
c1SPP	T-T^{3}PPD(5)P^{4}PCL(18,75)	300	244 ± 3	78.8 ± 0.2	99.8 ± 0.3	79 ± 0	21 ± 0	62 ± 1	84 ± 2
	T-T^{3}PPD(5)P^{4}PCL(18,50)	300	231 ± 5	76.9 ± 0.3	99.9 ± 1.1	78 ± 1	22 ± 1	60 ± 1	76 ± 2
	T-T^{3}PPD(5)P^{4}PCL(10,50)	300	222 ± 1	72.2 ± 0.3	99.7 ± 0.2	74 ± 2	26 ± 2	56 ± 2	83 ± 1
	T-T^{3}PPD(5)P^{4}PCL(5,50)	300	200 ± 4	64.8 ± 0.3	97.7 ± 0.5	73 ± 1	24 ± 1	48 ± 2	82 ± 1

[a] see Table 1 note a.

Submitted to ADVANCED FUNCTIONAL MATERIALS

The table of contents

Polymeric Materials, Shape-Memory Materials, Stimuli-Responsive Materials

J. Zotzmann, M. Behl, Y. Feng, A. Lendlein*

Copolymer Networks Based on Poly(ω-pentadecalactone)- and Poly(ε-caprolactone)-Segments as a versatile Triple-Shape Polymer System

The domains of multiphase copolymer networks obtained by linking star-shaped precursors having segments of poly(*ω*-pentadecalactone) (red) and poly(*ε*-caprolactone) (yellow) with an diisocyanate (black) acted as stimuli-sensitive switches, which enabled a triple-shape effect. This triple-shape effect could be obtained by two-step programming at T_{high} as well as a one-step deformation at T_{high} or, most impressively, at ambient temperature.

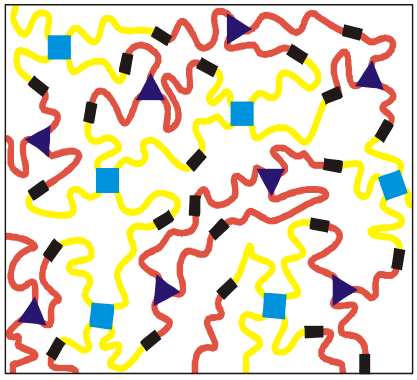

Submitted to ADVANCED FUNCTIONAL MATERIALS

Supporting Information

Table S1. Synthesis of star-shaped precursors: starting materials, number average molecular weight (M_n), glass transition temperature (T_g), and melting point (T_m).

precursor ID[a]	initiator ID[a]; m [g]	monomer ID[b]; m [g]	DBTO m [mg]	M_n[c] [g·mol^{-1}]	M_n[d] [g·mol^{-1}]	M_n[e] [g·mol^{-1}]	T_g[f] [°C]	T_m[f] [°C]
T^{3}PPD(5)	T^3; 5.00	PDL; 75	70	5100	3800	--	--	87
T^{3}PPD(3)	T^3; 5.00	PDL; 67	70	3400	3500	--	--	85
P^{4}PCL(18)	P^4; 0.68	CL; 100	280	17800	22700	23400	-61	54
P^{4}PCL(10)[g]	P^4	CL	--	9600	8400	10700	-65	53
P^{4}PCL(5)	P^4; 3.40	CL; 100	280	5400	4500	6300	-62	51

[a] T^{3}PPD(5) denotes the 3 arm star-shaped PPD precursor with M_n approximately 5000 g·mol^{-1} using 2-ethyl-2-(hydroxymethyl)propane-1,3-diol 6-hydroxycaproates (T^3) as initiator, P^{4}PCL(x) are 4 arm PCL precursors with the approximate M_n (x·1000 g·mol^{-1}) given in parenthesis using pentaerythritol (P^4) as initiator, [b] monomers are pentadecalactone (PDL) and –caprolactone (CL); [c] from GPC measurements; [d] calculated from measurements of the OH-number; [e] calculated from ^{1}H-NMR measurements, calculation for PPD precursors not impossible due to signal overlapping; [f] from DSC measurements; [g] commercial name: CAPA4801.

Table S2. Synthesis of polymer networks from T^{3}PPD(5), T^{3}PPD(3), P^{4}PCL(18), P^{4}PCL(10), and P^{4}PCL(5) by polyaddition with TMDI; starting materials, gel content (*G*), mass gain during swelling of the polymer networks in chloroform (*S*).

Sample ID[a]	μ_{PCL} [wt%]	T^{3}PPD *m* [g]	P^{4}PCL *m* [g]	TMDI *V* [ml]	*G*[b] [wt%]	*S*[b] [wt%]
T-P^{4}PCL(18)	100	--	3.00	0.074	88 ± 2	2160 ± 40
T-P^{4}PCL(10)	100	--	3.00	0.200	99 ± 1	740 ± 20
T-P^{4}PCL(5)	100	--	3.00	0.373	97 ± 1	1050 ± 20
T-T^{3}PPD(5)P^{4}PCL(18,75)	75	0.75	2.25	0.106	95 ± 1	1220 ± 30
T-T^{3}PPD(5)P^{4}PCL(18,60)	60	1.20	1.80	0.113	92 ± 2	1400 ± 50
T-T^{3}PPD(5)P^{4}PCL(18,50)	50	1.50	1.50	0.118	92 ± 2	1400 ± 40
T-T^{3}PPD(5)P^{4}PCL(18,40)	40	1.80	1.20	0.122	92 ± 1	1230 ± 90
T-T^{3}PPD(5)P^{4}PCL(18,25)	25	2.25	0.75	0.141	93 ± 2	1190 ± 80
T-T^{3}PPD(5)P^{4}PCL(10,75)	75	0.75	2.25	0.148	98 ± 1	900 ± 10
T-T^{3}PPD(5)P^{4}PCL(10,60)	60	1.20	1.80	0.146	96 ± 1	1100 ± 10
T-T^{3}PPD(5)P^{4}PCL(10,50)	50	1.50	1.50	0.145	97 ± 1	1040 ± 30
T-T^{3}PPD(5)P^{4}PCL(10,40)	40	1.80	1.20	0.144	92 ± 1	1580 ± 20
T-T^{3}PPD(5)P^{4}PCL(10,25)	25	2.25	0.75	0.143	91 ± 1	1580 ± 20
T-T^{3}PPD(5)P^{4}PCL(5,75)	75	0.75	2.25	0.260	98 ± 1	1010 ± 10
T-T^{3}PPD(5)P^{4}PCL(5,60)	60	1.20	1.80	0.236	96 ± 1	1110 ± 20
T-T^{3}PPD(5)P^{4}PCL(5,50)	50	1.50	1.50	0.220	96 ± 1	1100 ± 10
T-T^{3}PPD(5)P^{4}PCL(5,40)	40	1.80	1.20	0.204	97 ± 1	1010 ± 20
T-T^{3}PPD(5)P^{4}PCL(5,25)	25	2.25	0.75	0.180	93 ± 1	1350 ± 20
T-T^{3}PPD(5)	0	1.50	--	0.070	91 ± 1	1420 ± 30
T-T^{3}PPD(3)P^{4}PCL(18,75)	75	0.75	2.25	0.124	85 ± 1	2080 ± 30

T-T^{3}PPD(3)P^{4}PCL(18,60)	60	1.20	1.80	0.205	94 ± 1	1200 ± 20
T-T^{3}PPD(3)P^{4}PCL(18,50)	50	1.50	1.50	0.186	84 ± 1	1940 ± 20
T-T^{3}PPD(3)P^{4}PCL(18,40)	40	1.80	1.20	0.194	95 ± 1	1170 ± 30
T-T^{3}PPD(3)P^{4}PCL(18,25)	25	2.25	0.75	0.250	97 ± 1	990 ± 20
T-T^{3}PPD(3)P^{4}PCL(10,75)	75	0.75	2.25	0.200	98 ± 1	800 ± 20
T-T^{3}PPD(3)P^{4}PCL(10,60)	60	1.20	1.80	0.236	99 ± 1	750 ± 10
T-T^{3}PPD(3)P^{4}PCL(10,50)	50	1.50	1.50	0.238	97 ± 1	790 ± 20
T-T^{3}PPD(3)P^{4}PCL(10,40)	40	1.80	1.20	0.212	97 ± 1	990 ± 40
T-T^{3}PPD(3)P^{4}PCL(10,25)	25	2.25	0.75	0.275	98 ± 1	800 ± 10
T-T^{3}PPD(3)P^{4}PCL(5,75)	75	0.75	2.25	0.302	95 ± 1	1050 ± 10
T-T^{3}PPD(3)P^{4}PCL(5,60)	60	1.20	1.80	0.301	98 ± 1	840 ± 20
T-T^{3}PPD(3)P^{4}PCL(5,50)	50	1.50	1.50	0.306	96 ± 1	880 ± 20
T-T^{3}PPD(3)P^{4}PCL(5,40)	40	1.80	1.20	0.308	98 ± 1	770 ± 20
T-T^{3}PPD(3)P^{4}PCL(5,25)	25	2.25	0.75	0.309	97 ± 1	830 ± 30
T-T^{3}PPD(3)	0	3.00	--	0.294	98 ± 1	780 ± 10

[a] T-T^{3}PPD(x)P^{4}PCL(x,y) are thermosets (T) from T^{3}PPD(x) segments and P^{4}PCL(x) segments with the approximate M_n (x·1000 g·mol^{-1}) and μ_{PCL} (y wt%) given in parenthesis, T-T^{3}PPD(x) networks are PPD homopolymer networks whereas T-P^{4}PCL(x) homopolymer networks contain P^{4}PCL segments only, [b] average value of three measurements ± standard deviation.

Figure S3

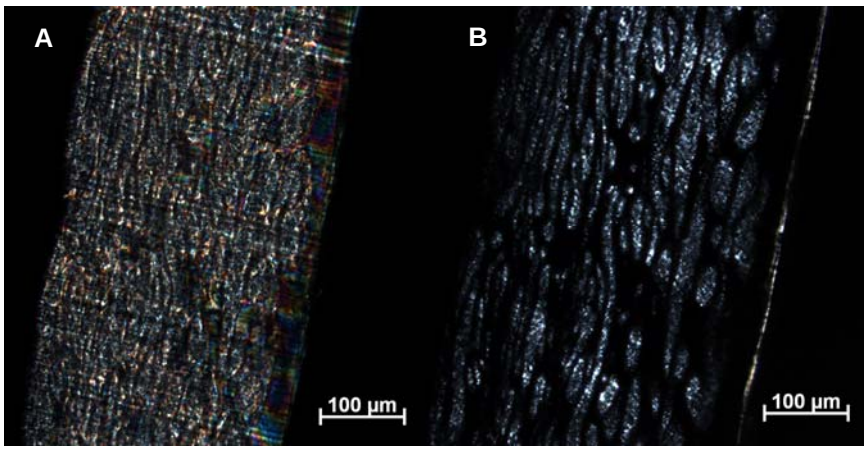

Figure S3. POM-pictures of a sample of T-T^{3}PPD(5)P^{4}PCL(18,50); A: at 28 °C; B: at 66 °C.

Figure S4

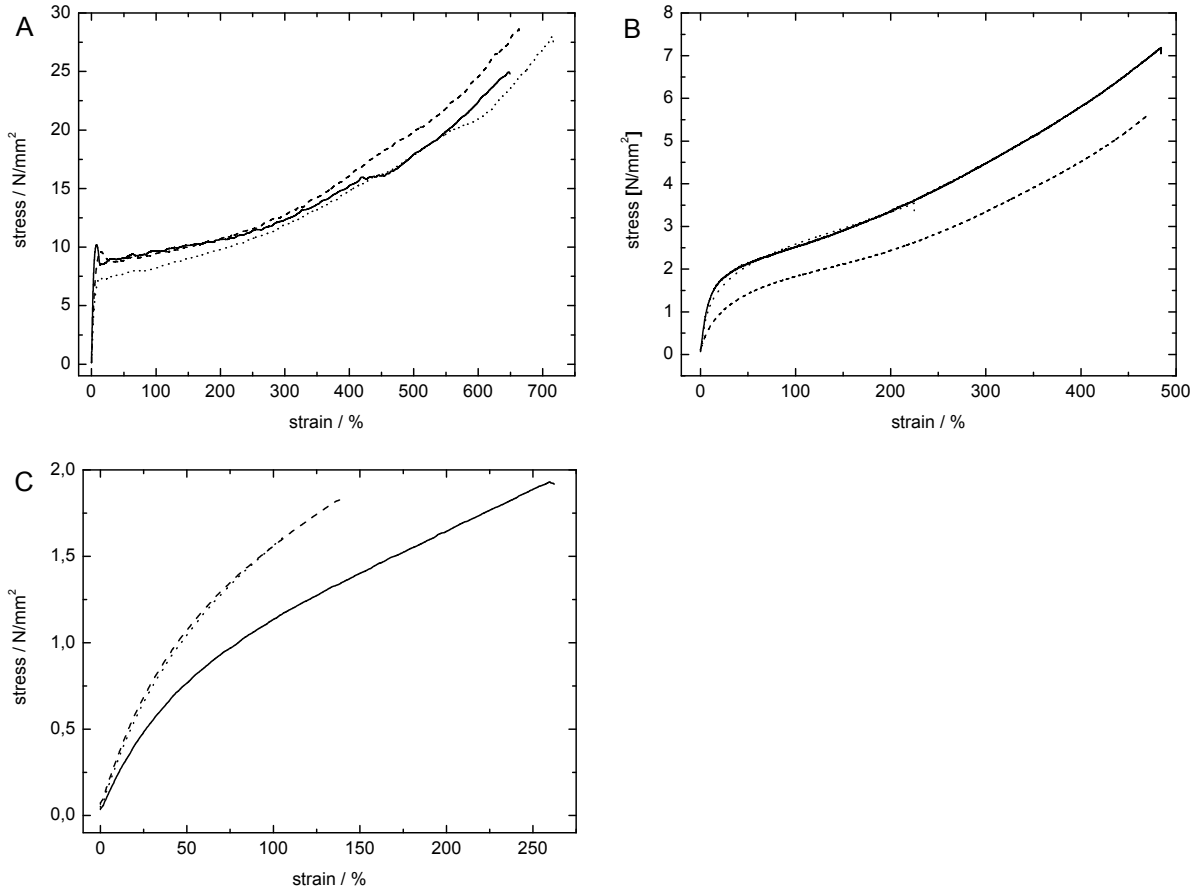

Figure S4. Typical stress-strain curves obtained from tensile test; A: at 25 °C; B: at 60 °C; C: at 100 °C; solid line: T-T^{3}PPD(5)P^{4}PCL(18,60), dashed line: T-T^{3}PPD(5)P^{4}PCL(10,60), dotted line: T-T^{3}PPD(5)P^{4}PCL(5,60).

Method S5:

The morphology pictures were taken on an AxioImager A1.m polarizing optical microscope (POM) equipped with an AxioCam MR3 camera (Carl Zeiss, Jena, Germany) and a LTS 350 hot stage (Linkam, Waterfield, UK) in the transmitted light mode with crossed polarization filters. The sample was prepared as histological cut with 30 μm thickness on a Cryotome Microm HM560 (Thermo Scientific, Walldorf, Germany) at -20 °C after embedding in paraffin. Heating/cooling rates of 1 K·min^{-1} were applied and the sample was 30 min equilibrated at the specific temperature before a picture was taken.